Applied Energy 370 (2024) 123638

Contents lists available at ScienceDirect

Applied Energy

journal homepage: www.elsevier.com/locate/apenergy

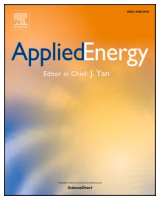

Lattice Boltzmann prediction of CO_2 and CH_4 competitive adsorption in shale porous media accelerated by machine learning for CO_2 sequestration and enhanced CH_4 recovery

Han Wang [a], Mingshan Zhang [b], Xuanzhe Xia [a], Zhenhua Tian [c], Xiangjie Qin [a], Jianchao Cai [a,*]

[a] National Key Laboratory of Petroleum Resources and Engineering, China University of Petroleum, Beijing 102249, China
[b] Key Laboratory of Ministry of Education on Safe Mining of Deep Metal Mines, School of Resources and Civil Engineering, Northeastern University, Shenyang 110819, China
[c] School of Geophysics and Geomatics, China University of Geosciences, Wuhan 430074, China

HIGHLIGHTS

- A methodology coupling with molecular simulation, lattice Boltzmann method and machine learning.
- Accurately and rapidly predicting CO_2-CH_4 competitive adsorption capacity in arbitrary large-scale porous media.
- Effects of shale mineral type and different CO_2 molar fractions were considered.

ARTICLE INFO

Keywords:
Shale gas
CO_2-CH_4 competitive adsorption
Lattice Boltzmann method
Machine learning
Artificial neural network

ABSTRACT

CO_2 injection has become the effective and potential means to enhance shale gas recovery and realize CO_2 geological sequestration because of the CO_2-CH_4 competitive adsorption. However, the clarification on CO_2-CH_4 competitive adsorption behaviors is mainly limited to molecular simulations based on single nanoscale pore size, and it is difficult to carry out large-scale calculations based on pore-scale simulations. In this study, a new methodology coupling with molecular simulation, lattice Boltzmann method and machine learning is proposed to accurately simulate and rapidly predict the CO_2-CH_4 competitive adsorption in kerogen and illite three-dimensional nanoporous media under different CO_2 molar fractions. From the features of pore structure and the accurate database of competitive adsorption behaviors from pore-scale simulations which are modified by molecular simulations, the Artificial Neural Network is then trained to be able to predict CO_2-CH_4 competitive adsorption capacity in arbitrary large-scale porous media. The above method overcomes the limitation of computing resource consumption of molecular simulation and pore-scale simulation, and provides research ideas and basic models for simulation and prediction of fluid adsorption behaviors in large-scale porous media.

1. Introduction

Shale gas, as a kind of clean energy, plays an indispensable role in the world's energy system [1,2]. In shale nanopores, because the sizes of the pore and fluid molecule are on the nanometer scale, the non-negligible and strong CH_4-surface interactions can result in the presence of a large amount of adsorbed gas [3,4], and the low fluidity of adsorbed gas has an important negative effect on shale gas production. Thanks to the greater adsorption capacity, the injected CO_2 can adsorb on different mineral surfaces and replace CH_4 from the adsorbed phase [5–11], thus becoming an effective means to enhance shale gas recovery, leading to an increase of more than 20% in shale gas production. Meanwhile, about 60% of the injected CO_2 is trapped in shale reservoirs [12], then, it is a potential way to reduce CO_2 emission and realize CO_2 geological sequestration [13]. Therefore, competitive adsorption is a dominant factor in enhancing shale gas recovery and realizing carbon geological sequestration through CO_2 huff-n-puff [14–16].

At present, the microscopic competitive adsorption mechanisms between hydrocarbons and CO_2 in different mineral nanoscale spaces have been investigated in detail through molecular dynamics simulation

* Corresponding author.
E-mail address: caijc@cup.edu.cn (J. Cai).

https://doi.org/10.1016/j.apenergy.2024.123638
Received 14 December 2023; Received in revised form 28 February 2024; Accepted 2 June 2024
Available online 8 June 2024

(MDS) [16–21]. Shale rocks are composed of minerals such as kerogen with different maturity, quartz, and clay, and the nanoscale space contributes to the CH_4 and CO_2 adsorptions [22–26]. The adsorption capacity of CO_2 on the mineral surface is generally 2–10 times that of CH_4 [27–29]. The CO_2-CH_4 competitive adsorption behaviors are influenced by many factors such as mineral type, kerogen maturity, pore size, pressure, temperature, CO_2 content, CO_2 injection velocity/pressure, pore structure, and water [10,11,30–33]. However, the current molecular simulations are mostly limited to single pore structures to qualitatively analyze the influence mechanisms of different factors. At the corner of special pore structures or when the pore size is small, the fluid density is greater than that near the flat wall owing to the superposition of fluid-solid forces [34,35]. Mu et al., 2022 studied the effects of pressure and pore size on the sorption distribution of gas on shale minerals, the results show that the near-wall density can increase with a smaller pore size because of the superposition of interactions from both sides of pore walls [36]. Therefore, the complicated pore structures in porous media have a nonnegligible effect on adsorption behaviors, which is difficult studied and characterized by molecular simulations.

Alternatively, pore-scale simulations can effectively capture the physical and chemical behaviors of multiphase and multicomponent fluids in complex pore structures [37–41]. At present, the lattice Boltzmann method (LBM), as a popular pore-scale simulation method, is modified and adopted to investigate the fluid adsorption behaviors in nanoscale space [42–44]. Guo et al., 2016 presented and validated a new Shan-Chen lattice Boltzmann (LB) model for physisorption [43], and only the fluid in the first lattice space near the wall was considered for adsorption behavior. Zhang et al., 2019 presented the convection-diffusion types LB considering dynamics sorption to model the fluid absorption in the solid matrix [42]. However, LB simulation cannot spontaneously simulate the real gas-solid interaction force, so some scholars have carried out pore-scale simulation by coupling molecular simulations. By modifying the gas-solid interaction forces through coupling MDS in the LB model, Zhao et al., 2016 studied the adsorption effects on gas storage and recovery [45]. Zhang et al., 2020 incorporated water-surface molecular interactions into Shan-Chen LB equations to capture the exponential change density distribution, and this model can also be extended for single-phase adsorption simulation [46]. Liu et al., 2021 adopted the velocity and density profiles simulated by MDS as reference data, and applied LB simulation to model the shale gas flow in nanopores [47]. However, the present researches are mainly limited to the adsorption characteristics of single-component fluid, without considering the competitive adsorption of multi-component fluids, such as shale gas and CO_2 on solid surfaces after CO_2 injection. Recently, Wu et al., 2023 modeled the CO_2 displacement of CH_4 in nanoporous media considering the CO_2 adsorption, however, it is the exchange of methane in the solid with CO_2 in the pore space, rather than the classical adsorption characteristic on shale mineral surfaces [48]. Liu et al., 2023 applied LBM to simulate the adsorption behavior of CH_4-CO_2 binary mixture by coupling multi-component GCMC simulations, however, this model is not suitable for adsorption behavior in complex pore structures [49]. In our previous study, we constructed a novel LBM to model oil-CO_2 competitive adsorption in two-dimensional (2D) porous media [34], in this work, this model will be extended to the competitive adsorption simulations in three-dimensional (3D) porous media.

LB simulations mainly focus on the qualitative research of physical and chemical behaviors in 2D porous media, while the quantitative research based on 3D porous media is still limited by the large resource consumption and calculation scale. At present, some scholars coupled direct simulation, indirect simulation, and machine learning to accelerate the calculation and prediction of fluid transport behaviors in porous media [50]. Rabbani et al., 2019 modeled fluid flow in a large number of pore-throat structures and calculated permeability, and then trained an Artificial Neural Network (ANN) to predict the conductance of fluid flow in arbitrary pore-throat structure in pore network model (PNM), and finally realize the fast and accurate calculation of porous media permeability [51]. Then, Zhao et al., 2020 extended the improved PNM into the two-phase flow and predicted relative permeability [52]. Afterward, Zhao et al., 2021 coupled the advantages of the lower computational cost of the PNM by considering the real pore structures and the accurate calculation of LBM, by calculating the conductance of fluid flow through different pore throat structures in the PNM by LBM, and then the permeability of porous media can be rapidly and accurately calculated [53]. Jiang et al., 2021 applied LB simulation to study the three-phase flow, and then used machine learning techniques to predict the permeability from the LB simulation database [50]. Aslannejad et al., 2022 coupled a LB-smoothed model and ANN to accurately simulate and predict the colloid transport [54]. The above researches mostly focus the conventional scale flow simulation and permeability prediction, which can be easily extended to the prediction of fluid flow behaviors in nanoscale space by coupling boundary slip, fluid-fluid slip, heterogeneous viscosity, and other properties in LBM. However, the above models are not suitable for extending to the simulation and prediction of competitive adsorption behaviors.

In this work, a coupled methodology of molecular simulation, LB simulation and machine learning is proposed to accurately simulate and rapidly predict CO_2-CH_4 competitive adsorption in 3D nanoporous media, and the different CO_2 molar fractions are considered. Firstly, several nanoporous media containing 2096 pore structures are randomly constructed, and the characteristic parameters of each pore structure are extracted. Subsequently, by fitting the density results from molecular simulations, LBM is modified and applied to accurately model the CO_2-CH_4 competitive adsorption in nanoporous media considering different CO_2 molar fractions and minerals, and the competitive adsorption capacity in each pore structure is calculated. Finally, based on the above simulation results, machine learning is used to rapidly predict the competitive adsorption capacity in arbitrary pore structures by a trained ANN.

2. Methodology

2.1. Construction of porous media and pore structures

The 14 random nanoporous media models with different pore structures are first constructed [55–57], and the pore space is divided into 2096 pore structures by the watershed segmentation algorithm. The lattice size of the 14 nanoporous media is $150 \times 150 \times 150$, and the corresponding physical size is $30 \times 30 \times 30$ nm^3. The solid matrix and storage space of a nanoporous media are shown in Fig. 1, and there are two pore-throat structures in the storage space while each includes two divided pore structures. Then, based on the grid number of each pore structure, the volume, solid surface area, and pore-throat surface area of 2096 pore structures can be calculated, which are regarded as the features for the following machine learning. The solid surface is the contact region between the gas and the solid mineral, and the pore-throat interface is the contact region of the fluid in different pore structures.

The three parameters of the volume, solid surface area, and pore-throat surface area are selected mainly for the following two reasons. The first reason is that the adsorption behavior is caused by the gas-solid molecular interaction force, so the solid surface area determines the region of the gas-solid force; The second reason is that compared with the slit nanopores used in molecular simulation, the pore structure in porous media is complex, and there are areas such as corners, which will cause the superposition of gas-solid molecular interaction forces and enhance the adsorption capacity [35]. While the pore structure volume and pore structure area (sum of solid surface and pore-throat surface area) reflect the complexity of the pore structure, that is, the smaller the ratio of pore structure volume to pore structure area, the more complex structures such as corners. Therefore, the above three parameters can fully reflect the effect of pore structure on competitive adsorption.

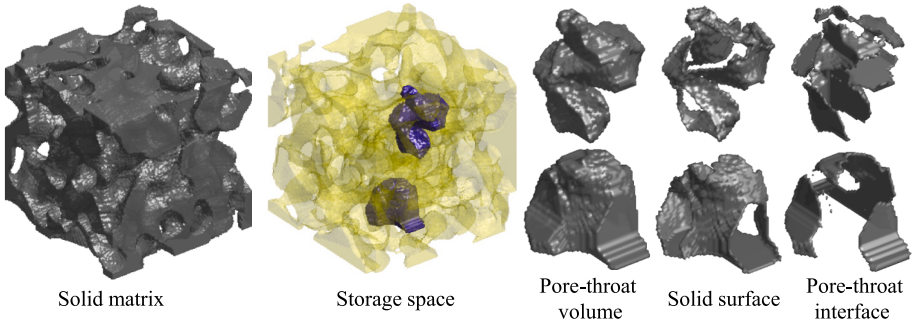

Fig. 1. Schematic diagram of nanoporous media, and the volume and surface region of pore structures.

2.2. Lattice Boltzmann simulation based on molecular simulation

Then, a multiphase and multicomponent Shan-Chen LBM coupling modified CO_2/oil-solid interaction force, proposed in our previous work [34], is extended to capture the CO_2-CH_4 competitive adsorption in 3D nanoporous media. The governing equation is given by

$$f_{\sigma,\alpha}(\mathbf{x}+\mathbf{e}_\alpha\delta_t, t+\delta_t) - f_{\sigma,\alpha}(\mathbf{x},t) = -\frac{1}{\tau}\left[f_{\sigma,\alpha}(\mathbf{x},t) - f^{eq}_{\sigma,\alpha}(\mathbf{x},t)\right], \quad (1)$$

where $f_{\sigma,\alpha=0,1,2,\ldots,18}(\mathbf{x},t)$ is the density distribution of σ component (represents CO_2 and CH_4) at direction α, position $\mathbf{x}$, and time t; $\mathbf{e}_\alpha$ is unit velocity; δ_t is the time step; τ is the relaxation time; $f^{eq}_{\sigma,\alpha}$ is the equilibrium density distribution.

The adsorption behaviors for a single component can be captured through modifying the gas-solid force, which can be defined as [46,58].

$$\mathbf{F}_{\sigma,\text{ads}}(\mathbf{x},t) = -G_{\sigma s}\psi(\mathbf{x},t)\sum_{\alpha} e^{-\mathbf{x}_\alpha/\lambda}\mathbf{e}_\alpha, \quad (2)$$

where $\mathbf{x}_\alpha$ is the distance from the wall in direction α; $G_{\sigma s}$ is the parameter of gas-solid force; λ is the parameter controlling the trend of the density distribution curve. Then, the competitive adsorption behaviors can be achieved by applying Eq. (2) to CO_2 and CH_4 at the same time, and different $G_{\sigma s}$ and λ values can be used to obtain different competitive adsorption capacities and adsorption trends with distance from the solid wall. Based on the above model, the competitive adsorption in nanoporous media can be simulated. However, LB simulation cannot spontaneously simulate the real liquid-solid interaction force, and it is necessary to assign the interaction force parameter manually. The challenge is how to select accurate parameter of gas-solid interaction force. Molecular simulation can accurately capture the intermolecular force, and characterize the CO_2-CH_4 competitive adsorption behavior. Therefore, the shortcomings of LB simulation can be effectively solved by fitting gas-solid interaction force parameters through molecular simulations.

The Grand Canonical Monte Carlo (GCMC) method is then adopted to simulate adsorption behaviors in kerogen and illite slit nanopores, respectively. The kerogen surfaces are constructed by compressing some kerogen units with a moveable graphene piston during an annealing simulation process. On the other hand, the illite models are created by replicating the unit cell in x and y directions. In addition, K^+ is added to balance the negatively charged surfaces due to isomorphic substitution when building illite nanopores. The detailed construction procedure of these two nanopores and parameter settings of GCMC simulations can be found in our previous simulation work [59]. The consistent valence force field (CVFF) force field [60] is used to model kerogen molecules, and illite is simulated by CLAYFF force field [61]. Both CH_4 and CO_2 molecules are described by the TraPPE force field [62,63]. Then the adsorption behaviors of CO_2 and CH_4 in the 4 nm slit kerogen and illite pores are simulated.

Based on the total mass of CO_2 and CH_4 in the 4 nm slit pore of molecular simulation, the initial density of CO_2 and CH_4 in LB simulation can be determined. Then, by perfectly fitting the density distributions from molecular simulations, the interaction force parameters of CO_2-solid G_{CO_2}, and CH_4-solid G_{CH_4} in LB simulation are obtained, and the fitting results are illustrated in Fig. 2(A). In order to ensure that the fitting parameters in 4 nm pore can well capture the competitive adsorption behavior in the pores with different pore sizes in nanoporous media, the same fitting parameters are used to carry out the competitive adsorption behavior in the 2 nm pore, and the successful fitting process can be found in our previous work [64]. Then, based on the fitting parameters, the competitive adsorption in 14 nanoporous media is accurately simulated. Figs. 2(B) and 2(C) show the CO_2-CH_4 density distributions in kerogen and illite nanoporous media. The gas density near the solid surface is greater than that in the bulk region, and the result is in accordance with the density profile from molecular simulations. Additionally, in the corner area of solid minerals (marked in a circle), or as the pore size is small (marked in a square), the adsorption density increases because of the superimposed effect of the gas-solid interaction force. Based on the density distributions in 14 nanoporous media, the CO_2-CH_4 adsorption capacity in 2096 pore structures of 14 nanoporous media can be calculated. The CO_2-CH_4 adsorption capacity is the CO_2-CH_4 molar content in the adsorption region, and the thickness of CO_2-CH_4 adsorption region equals 1.6 nm and 1.4 nm respectively according to the density distribution in Fig. 2(A). In LB simulation, the length scale $L_0 = 2\times10^{-10}$ m, mass scale $M_0 = 8\times10^{-27}$ kg and time scale $T_0 = 4\times10^{-15}$ s are applied to conduct the unit conversion between lattice units and physical units. Therefore, according to the lattice CO_2-CH_4 density $\rho_{lattice}$ at each grid, the physical mass $M_{physial}$ of CO_2 and CH_4 at each grid can be calculate by $M_{physial} = \rho_{lattice}L_0^3M_0$, and then the total molar content of the gas in each pore structures by summing the mass of all grids and molar mass. In addition, for CO_2 and CH_4 to be miscible, the CO_2-CH_4 interaction force parameter equals to 0, and the lattice viscosity all equal to 0.1 which will not affect the competitive adsorption.

2.3. Machine learning

Based on the database from LB simulations, machine learning is used to accurately and rapidly predict the CO_2-CH_4 adsorption capacity in arbitrary pore structures to reduce computational resources. According to the features of the volume, solid surface area, and pore-throat interface area of 2096 pore structures, the dependency of the CO_2-CH_4 adsorption capacity on these features is statistically analyzed. Fig. 3 shows the dependence of different features on adsorption capacity in kerogen nanoporous media, and the CO_2 molar fraction in CO_2-CH_4 mixtures equals 0.5, and there are certain correlations between the adsorption capacity and these features. Then, the stepwise regression coefficients (SRC) are calculated, which are given in Table 1, the higher the stepwise regression coefficient, the stronger the correlation between the adsorption capacity and these features. The results show that the relationship between adsorption capacity and these characteristics is great, and the solid surface area is the best-correlated variable, mainly

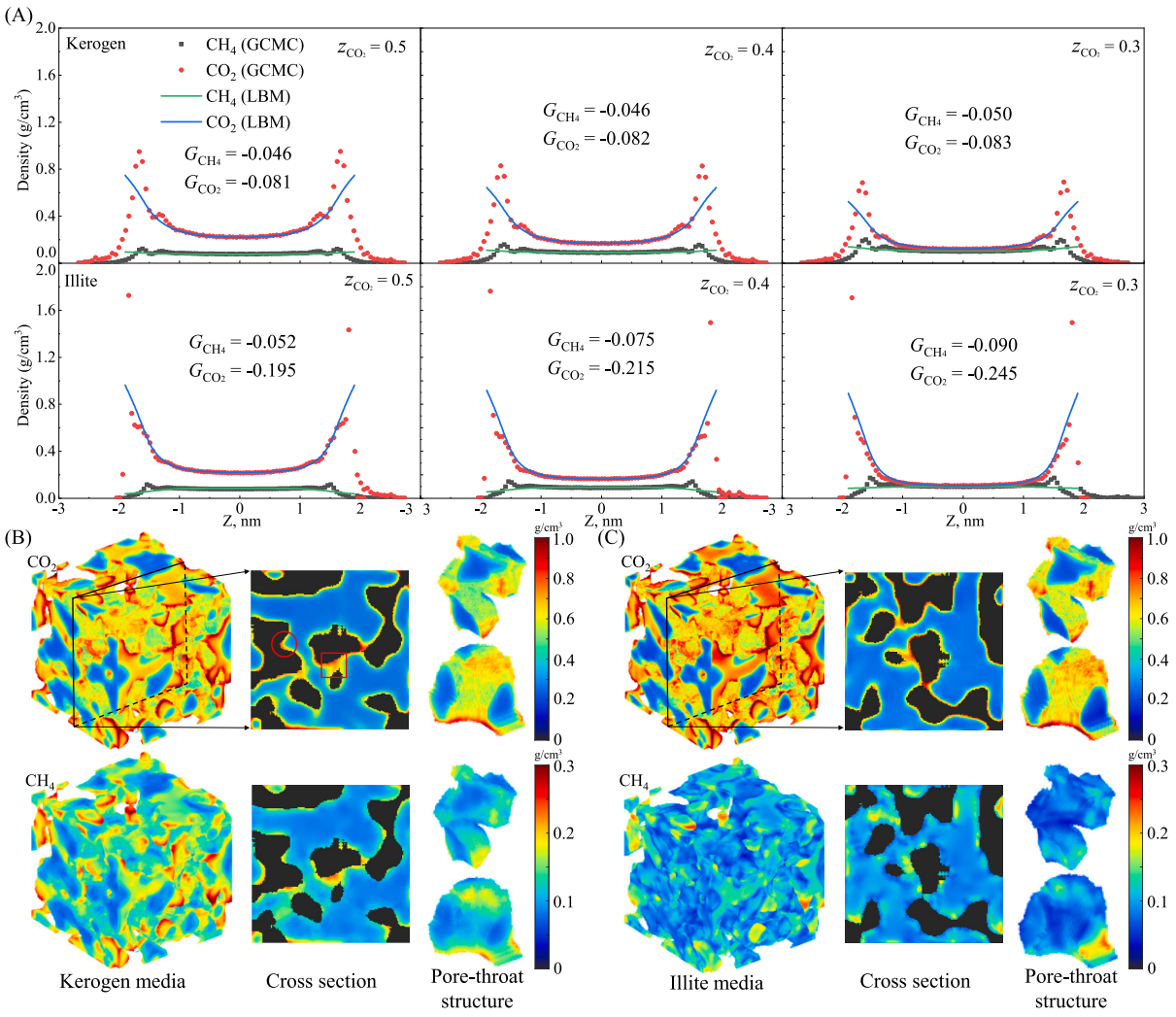

Fig. 2. CO_2 and CH_4 density distributions in kerogen and illite nanoporous media based on fitting molecular simulation results. (A) Parameters of adsorption in LB simulation are fitted by the density profiles from molecular simulations, and all simulations are conducted at a certain pressure (20 MPa) and temperature (333.15 K). (B) LB simulation on CO_2-CH_4 competitive adsorption in kerogen nanoporous media and pore structures, and the CO_2 molar fraction is 0.5. (C) LB simulation on CO_2-CH_4 competitive adsorption in illite nanoporous media and pore structures, and the CO_2 molar fraction is 0.5.

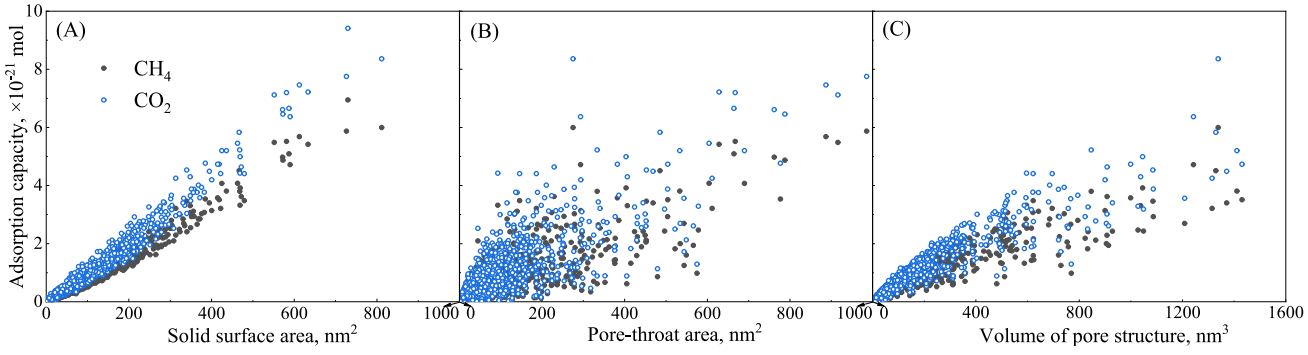

Fig. 3. Scatter diagrams of the relationship between features and adsorption capacity. (A) solid surface area, (B) pore-throat area, (C) Volume of pore structure.

Table 1
Stepwise regression coefficients between the features and adsorption capacity.

Feature	SRC of CH_4	SRC of CO_2
Solid area, nm^2	0.132	0.476
Pore-throat area, nm^2	0.091	0.332
Pore-throat volume, nm^3	0.043	0.157

because the adsorption behaviors are mainly caused by the strong gas-solid interaction force.

Then, the ANN with ReLu activation function, performed by the Neural Fitting Toolbox of MATLAB, is trained to be able to predict CO_2-CH_4 adsorption capacity in arbitrary pore structures. The ANN is trained with a single hidden layer and ten neurons in the hidden layer. The pore-structure volume, solid surface area, and pore-throat interface area are

input parameters, and CO_2-CH_4 adsorption capacity is the output parameter. The 5-fold cross validation is applied to guarantee the accuracy of ANN, and the mean squared error (MSE) and coefficient of determination (R^2) are used to evaluate the accuracy of the training. As given in Fig. 4, the results show that the ANN is able to predict adsorption behaviors with a small mean squared error (MSE = 0.0038) and high coefficient of determination (R^2 = 0.9974). We then reconstructed a new nanoporous media model with lattice size 150 × 150 × 150 and compared the ANN prediction with the pore-scale simulation. The results are shown in Fig. 5, which indicate the accuracy and reliability of the ANN predictions. Note: the above simulation results are used under the kerogen nanoporous media and CO_2 molar fraction equaling 0.5. In **Section 3**, we further conducted pore-scale simulations and neural network predictions for different minerals and different CO_2 molar fractions.

3. Results and discussion

3.1. Workflow of the competitive adsorption prediction

Molecular simulation, LB simulation, and machine learning are coupled to rapidly predict the CO_2-CH_4 competitive adsorption capacity in 3D nanoporous media. The main ideas of the coupled methodology are shown in Fig. 6 and as follows. 1). Simulating the competitive adsorption of CO_2-CH_4 mixtures in slit nanopores by molecular simulation, and calculating the density profiles. 2). Modifying the CH_4-solid and CO_2-solid interaction force parameters in LB simulation by fitting the competitive adsorption density profiles from molecular simulation. 3): Simulating the CO_2-CH_4 competitive adsorption in 3D nanoporous media with fitted gas-solid force parameters, and eventually obtaining the spatial density distributions of CO_2-CH_4 mixtures. 4): Dividing multiple 3D nanoporous media into 2096 pore structures by watershed segmentation algorithm, and calculating pore structure volume, solid surface area, and pore-throat surface area. Then, based on the spatial competitive adsorption density distribution, calculating the CO_2-CH_4 adsorption capacity in 2096 pore structures. 5): Building the databases of 2096 pore-structure features and CO_2-CH_4 adsorption capacity, and training ANN to predict the CO_2-CH_4 adsorption capacity in arbitrary pore structures. The above methodology can be well extended to the different shale reservoirs with different mineral composition and pore structures.

To highlight the computational efficiency of the proposed methodology, the computational time between the LB simulation and the ANN prediction is compared. The computational time of different LB programming methods is very different, in this work, Matlab is adopted to compile simulation programs without considering parallel calculation, and the program convergence takes about 5 h for the adsorption in one nanoporous media with lattice size 150 × 150 × 150. Regardless of the database preparation time, the prediction time based on the proposed methodology is less than 5 s. However, before the ANN prediction, a large number of simulations need to be carried out to conduct the database preparation. On the premise of ensuring sufficient pore structure, the different mineral types, CO_2 molar fractions, temperatures and pressures need to be considered, which greatly increases the workload. Moreover, the competitive adsorption behavior in large-scale porous media can be predicted, which is impossible to be directly simulated with current computing resources.

3.2. Machine learning considering mineral types and CO_2 molar fraction

Based on the above methodology, the competitive adsorption in 14 kerogen and illite nanoporous media with CO_2 molar fractions equaling 0.5, 0.4 and 0.3 are simulated, and the CO_2-CH_4 density distributions in 5 kerogen nanoporous media with CO_2 molar fractions equaling 0.3 and increasing pore size are shown in Fig. 7. Then, from the density distributions under the conditions of the different minerals (kerogen and illite), different CO_2 molar fractions (0.5, 0.4 and 0.3) and different pore structures (2096 samples), we build a database composed 12,576 entries for the CO_2-CH_4 adsorption capacity to train ANN to predict the competitive adsorption capacity in arbitrary pore structures with different minerals and CO_2 molar fractions. For the training, the mineral type, CO_2 molar fraction, the volume of pore structure, the solid surface area and pore-throat interface area are input parameters, and CO_2-CH_4 adsorption capacity is taken as output parameter. Fig. 8 indicates the training results of the CO_2-CH_4 adsorption capacity, and a reasonably high coefficient of determination ($R^2_{CO_2}$ = 0.99, $R^2_{CH_4}$ = 0.99) indicates the ANN has the ability to accurately predict the CO_2-CH_4 adsorption capacity in arbitrary pore structures.

3.3. Effect of pore size, CO_2 molar fraction and mineral type on competitive adsorption

Based on the predicted results, the influences of pore size, CO_2 molar fraction and mineral type on the CO_2-CH_4 adsorption capacity are discussed. First, the 10 nanoporous media models with monotonically increasing aperture and the same porosity are established, and some nanoporous media models are given in Fig. 9. The lattice size of nanoporous media model is 300 × 300 × 300, and the corresponding physical size is 60 × 60 × 60 nm^3, in addition, the porosity is constant and equals to 0.5. Then, through the watershed segmentation algorithm, the nanoporous media models are divided into a large number of pore structures, and the training results in **section 3.2** are applied to predict the CO_2-CH_4 adsorption capacity in pore structures. The predicted results in kerogen nanoporous media with average pore diameter equaling 3.6 nm, 4.6 nm and 5.4 nm are indicated in Fig. 10. The results indicate that with increasing pore size, the volume and solid surface area of pore structures increase, resulting in the increase of CO_2-CH_4 adsorption capacity.

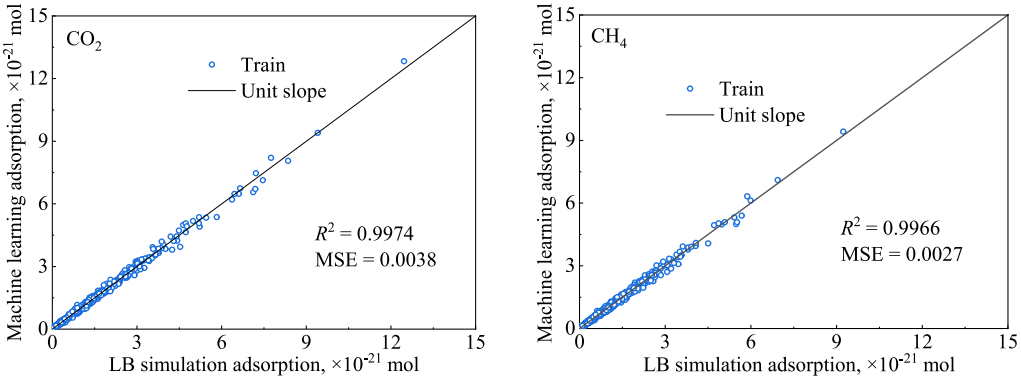

Fig. 4. The capability of ANN to predict CO_2-CH_4 adsorption capacity.

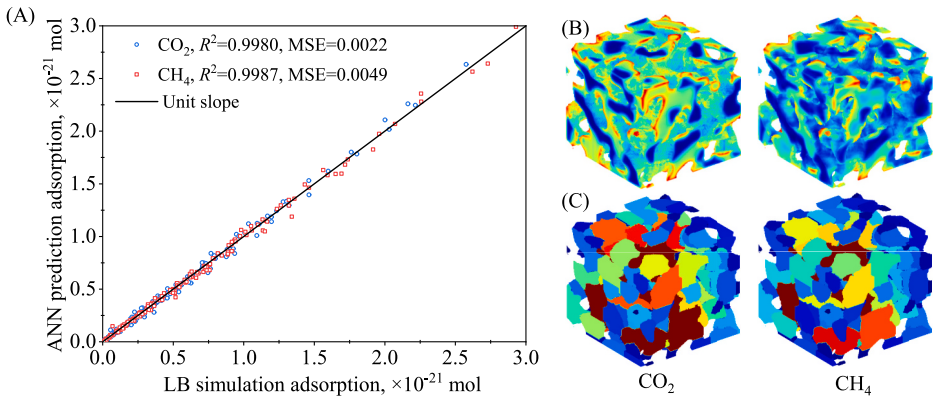

Fig. 5. The comparation of adsorption capacity between ANN prediction and LB simulation. (A) The comparation of adsorption capacity; (B) Density distribution in nanoporous media from LB simulation; (C) Total adsorption capacity in each pore structure in nanoporous media from ANN prediction, and the color from blue to red indicates a gradual increase in the total adsorption capacity in pore structures. (For interpretation of the references to color in this figure legend, the reader is referred to the web version of this article.)

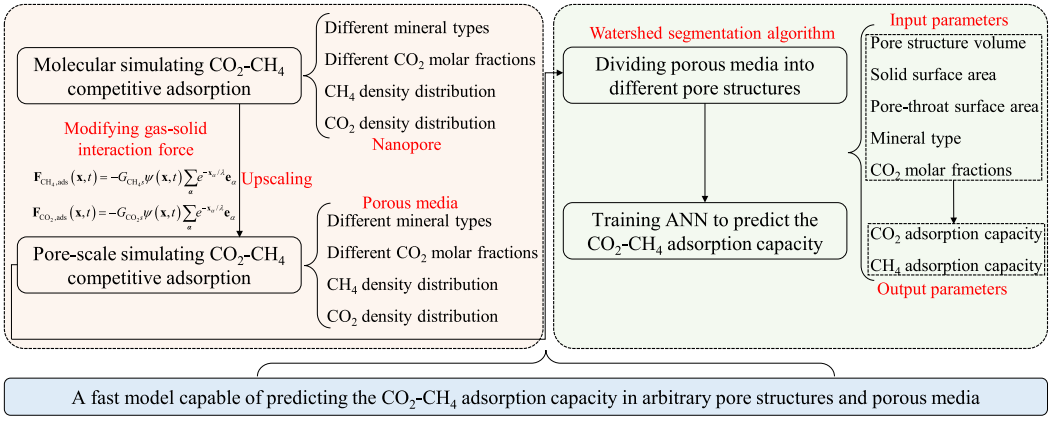

Fig. 6. Workflow of methodology.

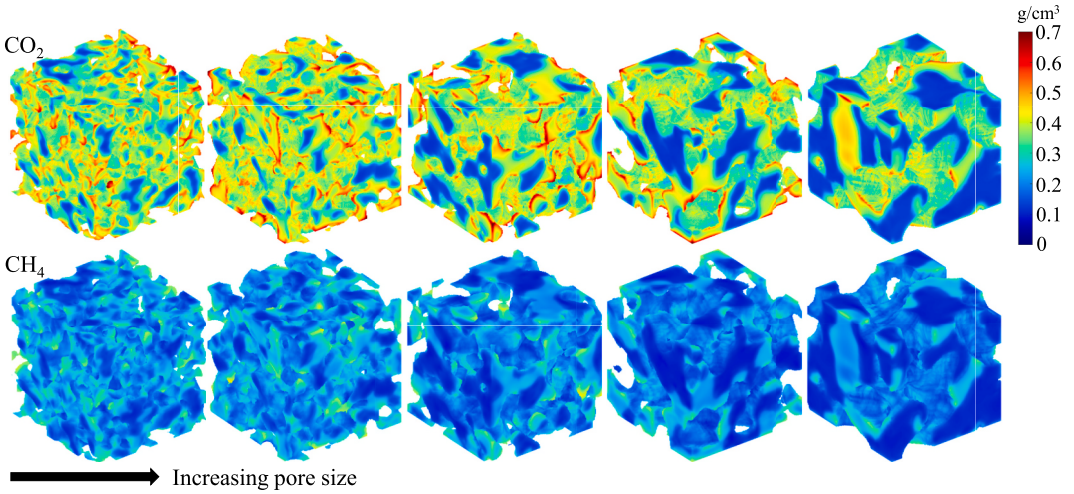

Fig. 7. CO_2-CH_4 density distribution in kerogen nanoporous media with different pore sizes.

The dependence of average pore size and CO_2 molar fraction on CO_2-CH_4 adsorption capacity in kerogen nanoporous media is indicated in Fig. 11. The increasing pore size makes for the decreasing specific surface area, and thus the decreasing gas-solid contact area which dominates the adsorption. Additionally, in the pore structure with a small pore size, the superposition of gas-solid interaction force leads to more adsorption such as that at the corner of the pore. For this reason, when the pore size increases, the CO_2-CH_4 adsorption capacity decreases. It is consistent with the adsorption capacity in nanoporous media in Fig. 10, with the increase of CO_2 molar fraction, the adsorption capacity of CO_2 increases while that of CH_4 decreases.

The effects of mineral types on the CO_2-CH_4 adsorption capacity are

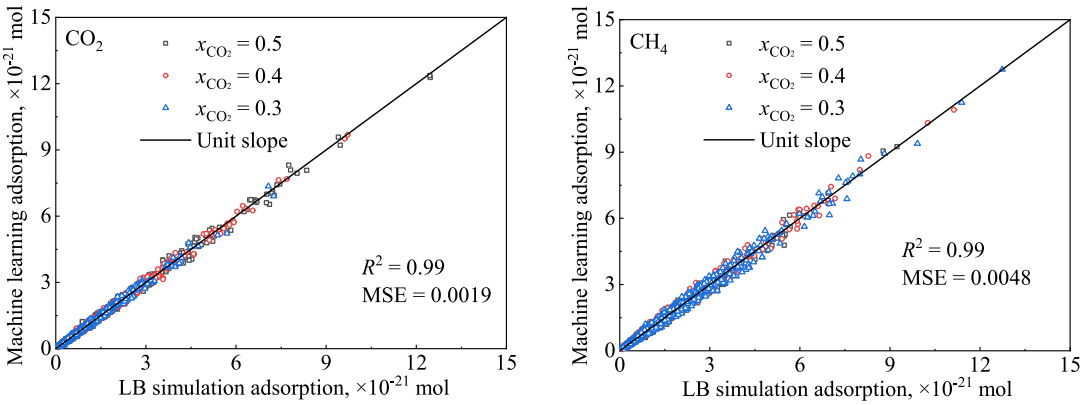

Fig. 8. The capability of ANN to predict CO_2-CH_4 adsorption capacity in kerogen and illite nanoporous media under different CO_2 molar fractions.

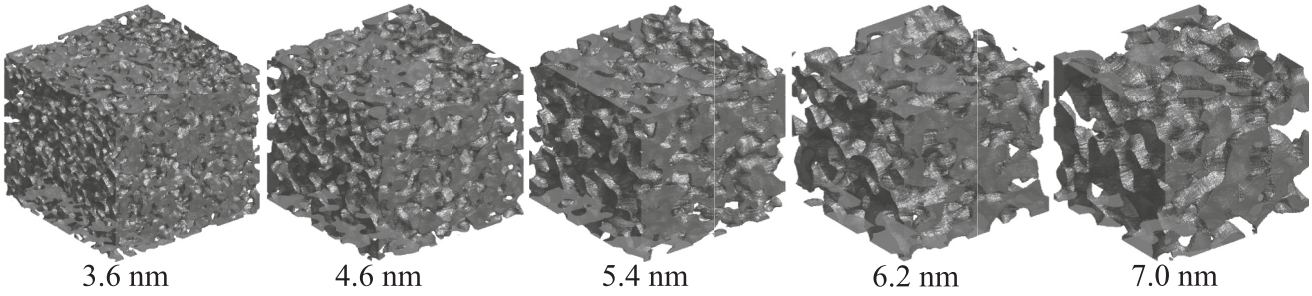

Fig. 9. Nanoporous media with different pore diameters. The average pore diameters are 3.6 nm, 4.6 nm, 5.4 nm, 6.2 nm and 7.0 nm respectively.

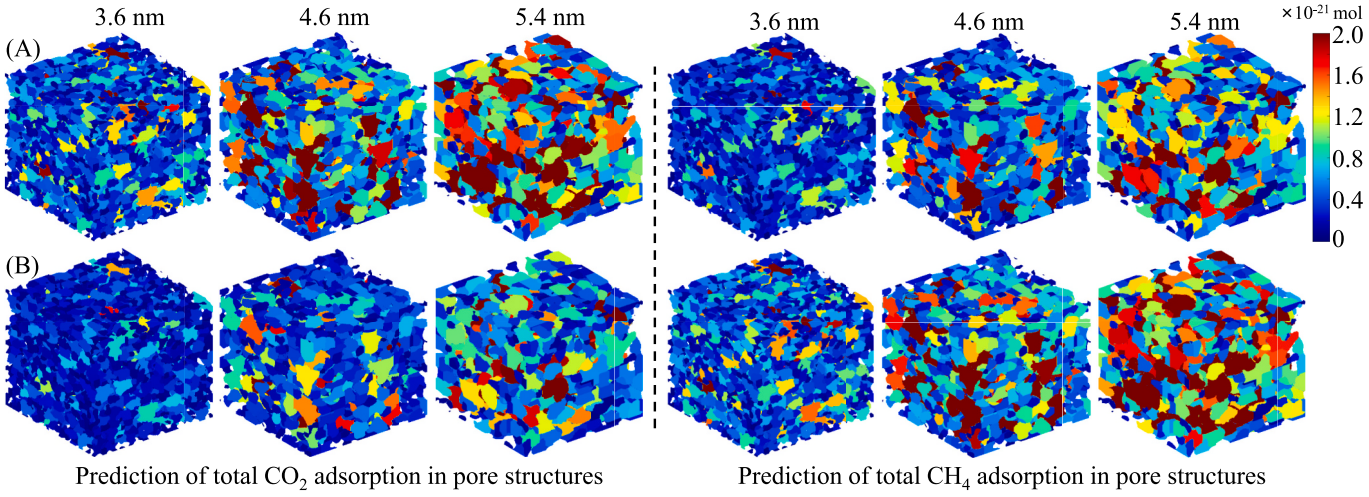

Fig. 10. Prediction of total CO_2-CH_4 competitive adsorption capacity. (A)$x_{CO_2} = 0.5$, (B)$x_{CO_2} = 0.3$.

shown in Fig. 12. As the pore size increases, the CO_2 adsorption capacity in kerogen and illite nanoporous media is a bit different under different CO_2 molar fractions. The CH_4 adsorption capacity in kerogen media is greater than that in illite media, and the difference decreases with the increase of CO_2 molar fraction.

4. Conclusions

In this work, a coupled methodology of molecular simulation, LB simulation and machine learning is proposed to accurately and rapidly predict the CO_2-CH_4 competitive adsorption capacity in nanoporous media under different CO_2 molar fractions and shale mineral types. First, based on the accurate CO_2-CH_4 competitive adsorption behaviors calculated by molecular simulation, the CH_4-solid and CO_2-solid force parameters in LB simulation are modified, and the competitive adsorption simulations in 3D kerogen and illite nanoporous media under different CO_2 molar fractions are carried out. Then, the several 3D nanoporous media are divided into a large number of pore structures by watershed segmentation algorithm, and the different features and competitive adsorption capacity of pore structures are obtained statistically for training the ANN to be able to predict CO_2-CH_4 adsorption capacity in arbitrary pore structures. Finally, based on training results, the effects of pore size, CO_2 molar fraction, and mineral types on competitive adsorption capacity are discussed. The results show that the proposed methodology can accurately and quickly capture the competitive adsorption behavior in complex pore structures compared

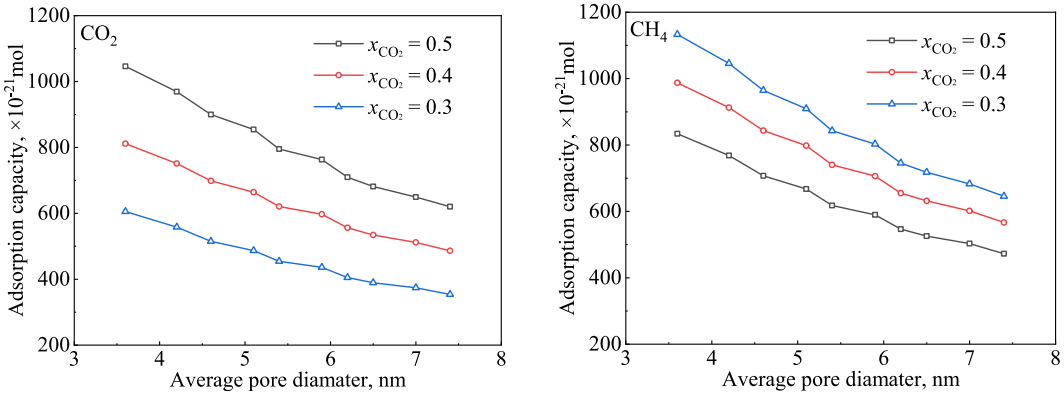

Fig. 11. The dependence of pore size and CO_2 molar fraction on the CO_2-CH_4 adsorption capacity in kerogen nanoporous media.

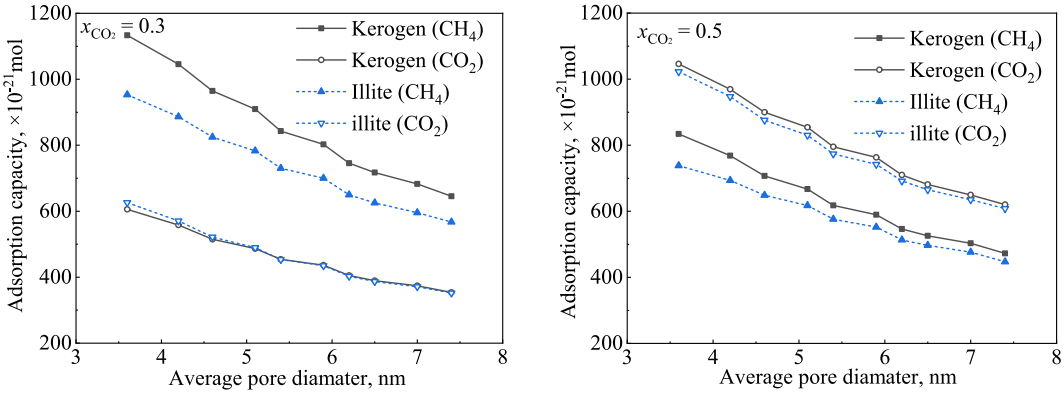

Fig. 12. CO_2-CH_4 adsorption capacity vs mineral types under different CO_2 molar fractions.

with the molecular simulation based on single nanopore. Because of the increasing specific surface area and the superposition of gas-solid interaction force, the CO_2-CH_4 adsorption capacity increases with decreasing pore size. With the increase of CO_2 molar fraction, the CO_2 adsorption increases while the CH_4 adsorption capacity decreases. The CO_2 adsorption capacity in kerogen and illite nanoporous media is a bit different while the CH_4 adsorption capacity in kerogen media is greater than that in illite media.

The above methodology overcomes the limitation of computing resource consumption based on single nanopore molecular simulation and porous media pore-scale simulation. Based on this methodology, we can predict the competitive adsorption behavior in a large number of porous media and then study the effects of coordination number, porosity, average pore size and other parameters on the competitive adsorption behaviors, to provide new phenomena that cannot be captured by molecular and pore-scale simulations. In addition, the reservoir can be divided into several porous media grids, and then the occurrence of CO_2-CH_4 in each porous media is predicted to eventually obtain the macroscopic spatial distribution of CO_2-CH_4 in reservoir. Therefore, this methodology can not only explain the competitive adsorption behavior from the microscopic aspect, but also be scaled up to the reservoir scale, which provides certain guiding significance for the formulation of CO_2 huff-n-puff to enhance shale gas recovery. As a basic model, this methodology can be extended to calculate CO_2 geological sequestration and underground hydrogen storage in shale nanoporous media accurately and rapidly (introduced in **Appendix A)**. By coupling PNM, the proposed method can also be extended to quickly calculate the permeability of nanoporous media considering the adsorption effect (introduced in **Appendix B)**.

CRediT authorship contribution statement

Han Wang: Writing – review & editing, Writing – original draft, Software, Project administration, Methodology, Investigation, Funding acquisition, Formal analysis, Data curation, Conceptualization. **Mingshan Zhang:** Formal analysis, Investigation, Methodology, Visualization, Writing – original draft. **Xuanzhe Xia:** Validation, Methodology, Formal analysis, Writing – original draft. **Zhenhua Tian:** Methodology, Software, Validation. **Xiangjie Qin:** Data curation, Formal analysis, Writing – original draft. **Jianchao Cai:** Conceptualization, Funding acquisition, Methodology, Supervision, Writing – review & editing.

Declaration of competing interest

The authors declare that they have no known competing financial interests or personal relationships that could have appeared to influence the work reported in this paper.

Data availability

Data will be made available on request.

Acknowledgment

We would also like to acknowledge funding support from the National Natural Science Foundation of China (No. 42172159), China Postdoctoral Science Foundation (Nos. 2023M733872 and 2023M730522), Postdoctoral Fellowship Program of CPSF (No. GZB20230864), and Science Foundation of China University of Petroleum, Beijing (No. 2462023XKBH009). The authors also thank Daowu Zhai for the guidance on machine learning.

Appendix A. CO_2 sequestration and hydrogen storage

Underground hydrogen storage has been identified as an effective solution for hydrogen storage, and due to the great adsorption capacity of hydrogen on mineral surface, shale reservoir is a potential carrier for hydrogen storage. Recently, Zhang et al., 2024 studied the hydrogen adsorption behaviors in shale kerogen and montmorillonite (MMT) nanopores through molecular simulation, and calculated the density distribution of pure hydrogen, as given in Fig. A1 [65]. Based on the proposed methodology, the parameters in pore-scale simulation can be fitted by hydrogen density distribution, and then coupling machine learning, the storage characteristics and storage quality of hydrogen in the shale porous media can be accurately and rapidly predicted.

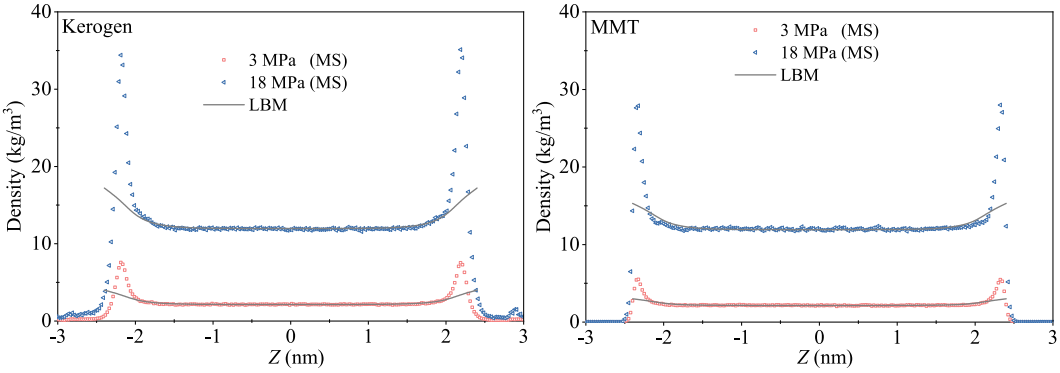

Fig. A1. LB and molecular simulation density distributions of pure hydrogen in kerogen and MMT nanopores.

Appendix B. Calculation of permeability

As shown in Fig. B1, the shapes of kerogen pores are diverse according to SEM images [66], however, unlike circle, square and slit pores, the physical behavior of fluid in irregularly shaped pores is difficult to characterize theoretically, and it is difficult to obtain physical models of pores with different shapes in molecular simulations. To overcome the above difficulties, the methodology presented in this paper can be used to rapidly predict competitive adsorption and flow behaviors.

First, the competitive adsorption behavior of CO_2 and CH_4 in a large number of pores with different shapes can be simulated, and the CO_2 density in kerogen nanopores with CO_2 molar fraction equaling 0.5 is shown in Fig. B2. Then, the nanoscale LBM [35,67] can be used to simulate the flow behaviors and calculate the permeability in the pores with different shapes, and the velocity distribution in the pores is shown in Fig. B2. Based on the database of competitive adsorption capacity and permeability obtained by direct simulations, the PNM and machine learning method can then be coupled to rapidly predict the competitive adsorption behavior and permeability in arbitrary nanoporous media at the same time.

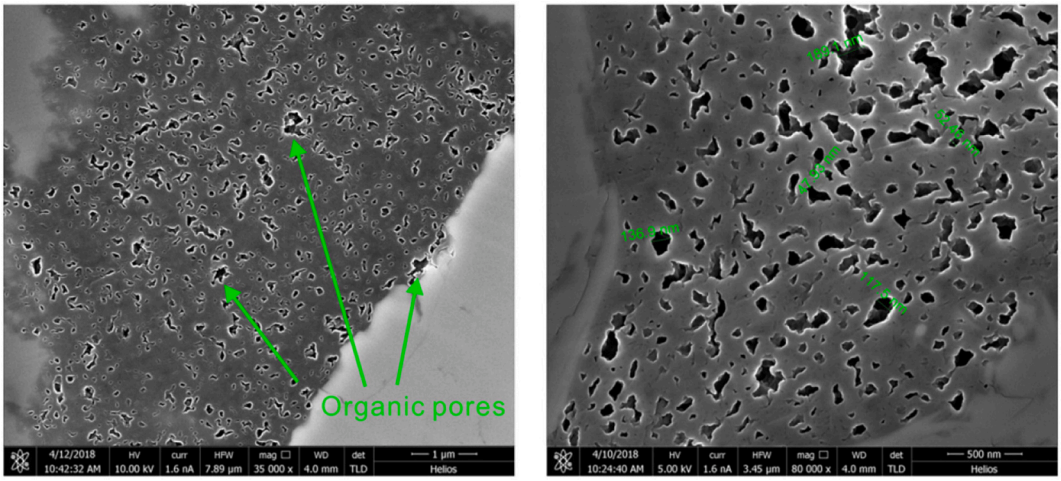

Fig. B1. SEM images of kerogen pores with arbitrary shapes of pore cross-section [66].

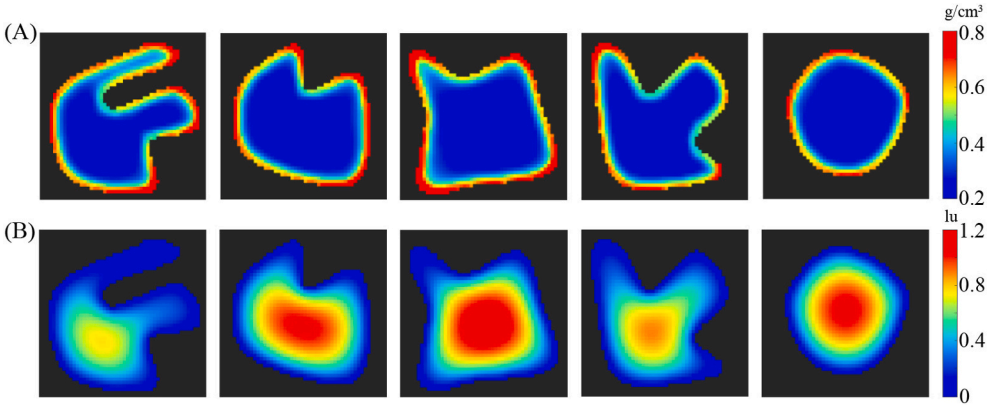

Fig. B2. Density (A) and velocity (B) distributions in nanopores with different pore shapes.

References

[1] Natural gas explained Where our natural gas comes from. https://wwweiagov/energyexplained/natural-gas/where-our-natural-gas-comes-fromphp; 2024.
[2] Natural Gas Annual. https://wwweiagov/naturalgas/annual/; 2024.
[3] Umeozor EC, Jordaan SM, Gates ID. On methane emissions from shale gas development. Energy 2018;152:594–600.
[4] Klewiah I, Berawala DS, Walker HCA, Andersen PØ, Nadeau PH. Review of experimental sorption studies of CO_2 and CH_4 in shales. J Nat Gas Sci Eng 2020;73:103045.
[5] Zhou J, Jin Z, Luo KH. Insights into recovery of multi-component shale gas by CO_2 injection: a molecular perspective. Fuel 2020;267:117247.
[6] Wang T, Tian S, Li G, Sheng M, Ren W, Liu Q, et al. Molecular simulation of CO_2/CH_4 competitive adsorption on shale kerogen for CO_2 sequestration and enhanced gas recovery. J Phys Chem C 2018;122(30):17009–18.
[7] Wu H, Jin Z, Xu X, Zhao S, Liu H. Effect of competitive adsorption on the deformation behavior of nanoslit-confined carbon dioxide and methane mixtures. Chem Eng J 2022;431:133963.
[8] Xie W, Wang M, Chen S, Vandeginste V, Yu Z, Wang H. Effects of gas components, reservoir property and pore structure of shale gas reservoir on the competitive adsorption behavior of CO_2 and CH_4. Energy 2022;254:124242.
[9] Liu B, Qi C, Mai T, Zhang J, Zhan K, Zhang Z, et al. Competitive adsorption and diffusion of CH_4/CO_2 binary mixture within shale organic nanochannels. J Nat Gas Sci Eng 2018;53:329–36.
[10] Iddphonce R, Wang J. Investigation of CO_2 and CH_4 competitive adsorption during enhanced shale gas production. J Pet Sci Eng 2021;205:108802.
[11] Huang L, Ning Z, Wang Q, Zhang W, Cheng Z, Wu X, et al. Effect of organic type and moisture on CO_2/CH_4 competitive adsorption in kerogen with implications for CO_2 sequestration and enhanced CH4 recovery. Appl Energy 2018;210:28–43.
[12] Iddphonce R, Wang J, Zhao L. Review of CO_2 injection techniques for enhanced shale gas recovery: Prospect and challenges. J Nat Gas Sci Eng 2020;77:103240.
[13] Kim TH, Cho J, Lee KS. Evaluation of CO_2 injection in shale gas reservoirs with multi-component transport and geomechanical effects. Appl Energy 2017;190:1195–206.
[14] Liao Q, Zhou J, Xian X, Yang K, Zhang C, Dong Z, et al. Competition adsorption of CO_2/CH_4 in shale: implications for CO_2 sequestration with enhanced gas recovery. Fuel 2023;339:127400.
[15] Jeong SR, Park JH, Lee JH, Jeon PR, Lee C-H. Review of the adsorption equilibria of CO_2, CH_4, and their mixture on coals and shales at high pressures for enhanced CH_4 recovery and CO_2 sequestration. Fluid Phase Equilib 2023;564:113591.
[16] Babatunde KA, Negash BM, Mojid MR, Ahmed TY, Jufar SR. Molecular simulation study of CO_2/CH_4 adsorption on realistic heterogeneous shale surfaces. Appl Surf Sci 2021;543:148789.
[17] Chong L, Myshakin EM. Molecular simulations of competitive adsorption of carbon dioxide–methane mixture on illitic clay surfaces. Fluid Phase Equilib 2018;472:185–95.
[18] Bonnaud PA, Oulebsir F, Galliero G, Vermorel R. Modeling competitive adsorption and diffusion of CH_4/CO_2 mixtures confined in mature type-II kerogen: insights from molecular dynamics simulations. Fuel 2023;352:129020.
[19] Moh DY, Zhang H, Wang S, Yin X, Qiao R. Soaking in CO_2 huff-n-puff: a single-nanopore scale study. Fuel 2022;308:122026.
[20] Zhang J, Liu K, Clennell M, Dewhurst D, Pervukhina M. Molecular simulation of CO_2–CH_4 competitive adsorption and induced coal swelling. Fuel 2015;160:309–17.
[21] Wu Z, Sun Z, Shu K, Jiang S, Gou Q, Chen Z. Mechanism of shale oil displacement by CO_2 in nanopores: a molecular dynamics simulation study. Adv Geo-Energy Res 2024;11(2):141–51.
[22] Xu S, Yassin MR, Dehghanpour H, Kolbeck C. The effects of kerogen maturity on pore structure and wettability of organic-rich calcareous shales. J Mol Liq 2022;362:119577.
[23] Begum M, Yassin MR, Dehghanpour H, Alberta U. Effect of kerogen maturity on organic shale wettability: a Duvernay case study. Mar Pet Geol 2019;110:483–96.
[24] Saraji S, Piri M. The representative sample size in shale oil rocks and nano-scale characterization of transport properties. Int J Coal Geol 2015;146:42–54.
[25] Rexer TF, Mathia EJ, Aplin AC, Thomas KM. High-pressure methane adsorption and characterization of pores in Posidonia shales and isolated kerogens. Energy Fuel 2014;28(5):2886–901.
[26] Glatz G, Alafnan S, Raza A, Mahmoud M. Multicomponent gas adsorption behavior of kerogen: a molecular investigation. Energy Fuel 2022;36(13):6695–710.
[27] Bekeshov D, Ashimov S, Wang Y, Wang L. Understanding gas-enhanced methane recovery in graphene nanoslits via molecular simulations. Capillarity 2023;6(1):1–12.
[28] Guo H, Wang Z, Wang B, Zhang Y, Meng H, Sui H. Molecular dynamics simulations of oil recovery from dolomite slit nanopores enhanced by CO_2 and N_2 injection. Adv Geo-Energy Res 2022;6(4):306–13.
[29] Zhou W, Wang H, Yang X, Liu X, Yan Y. Confinement effects and CO_2/CH_4 competitive adsorption in realistic shale kerogen nanopores. Ind Eng Chem Res 2020;59(14):6696–706.
[30] Hu X, Deng H, Lu C, Tian Y, Jin Z. Characterization of CO_2/CH_4 competitive adsorption in various clay minerals in relation to shale gas recovery from molecular simulation. Energy Fuel 2019;33(9):8202–14.
[31] Lu T, Zeng K, Jiang P, Zhou B, Xu R. Competitive adsorption in CO_2 enhancing shale gas: low-field NMR measurement combined with molecular simulation for selectivity and displacement efficiency model. Chem Eng J 2022;440:135865.
[32] Gomaa I, de Araujo IS, Heidari Z, Espinoza DN. Molecular simulation study of the competitive adsorption of carbon dioxide and methane in organic shale–implication for enhanced gas recovery. In: SPE/AAPG/SEG Unconventional Resources Technology Conference. URTEC; 2023. D011S9R01.
[33] Samara H, Ostrowski T, Abdulkareem FA, Padmanabhan E, Jaeger P. Carbon dioxide adsorption and interaction with formation fluids of Jordanian unconventional reservoirs. J Pet Explor Prod Technol 2021:1–13.
[34] Wang H, Su Y, Wang W, Jin Z, Chen H. CO_2-oil diffusion, adsorption and miscible flow in nanoporous media from pore-scale perspectives. Chem Eng J 2022;450:137957.
[35] Wang H, Su Y, Wang W. Improved lattice Boltzmann method to simulate liquid flow in nanoporous media: coupling molecular dynamics simulations and theoretical model. Adv Water Resour 2022;165:104239.
[36] Mu Z, Ning Z, Lyu F, Liu B. Sorption of deep shale gas on minerals and organic matter from molecular simulation. Energy Fuel 2022;37(1):251–9.
[37] Chen L, He A, Zhao J, Kang Q, Li Z-Y, Carmeliet J, et al. Pore-scale modeling of complex transport phenomena in porous media. Prog Energy Combust Sci 2022;88:100968.
[38] Yoon H, Kang Q, Valocchi AJ. Lattice Boltzmann-based approaches for pore-scale reactive transport. Rev Mineral Geochem 2015;80(1):393–431.
[39] Sadeghnejad S, Enzmann F, Kersten M. Digital rock physics, chemistry, and biology: challenges and prospects of pore-scale modelling approach. Appl Geochem 2021;131:105028.
[40] Chen L, Kang Q, Robinson BA, He Y-L, Tao W-Q. Pore-scale modeling of multiphase reactive transport with phase transitions and dissolution-precipitation processes in closed systems. Phys Rev E 2013;87(4):043306.
[41] Liu Y, Berg S, Ju Y, Wei W, Kou J, Cai J. Systematic investigation of corner flow impact in forced imbibition. Water Resour Res 2022;58(10):e2022WR032402.
[42] Zhang T, Sun S. A coupled lattice Boltzmann approach to simulate gas flow and transport in shale reservoirs with dynamic sorption. Fuel 2019;246:196–203.
[43] Guo L, Xiao L, Shan X, Zhang X. Modeling adsorption with lattice Boltzmann equation. Sci Rep 2016;6(1):1–9.
[44] Xu R, Prodanović M, Landry CJ. Study of subcritical and supercritical gas adsorption behavior in different nanopore systems in shale using lattice Boltzmann method. Int J Coal Geol 2019;212:103263.

[45] Zhao J, Yao J, Zhang L, Sui H, Zhang M. Pore-scale simulation of shale gas production considering the adsorption effect. Int J Heat Mass Transf 2016;103:1098–107.
[46] Zhang T, Javadpour F, Li X, Wu K, Li J, Yin Y. Mesoscopic method to study water flow in nanochannels with different wettability. Phys Rev E 2020;102(1):013306.
[47] Liu L, Wang Y, Aryana SA. Insights into scale translation of methane transport in nanopores. J Nat Gas Sci Eng 2021;96:104220.
[48] Wu J, Gan Y, Shi Z, Huang P, Shen L. Pore-scale lattice Boltzmann simulation of CO_2-CH_4 displacement in shale matrix. Energy 2023;127991.
[49] Liu L, Zhao Y, Luo M, Zhang L, Aryana SA. Bridging adsorption behavior of confined CH_4-CO_2 binary mixtures across scales. Fuel 2023;354:129310.
[50] Jiang F, Yang J, Boek E, Tsuji T. Investigation of viscous coupling effects in three-phase flow by lattice Boltzmann direct simulation and machine learning technique. Adv Water Resour 2021;147:103797.
[51] Rabbani A, Babaei M. Hybrid pore-network and lattice-Boltzmann permeability modelling accelerated by machine learning. Adv Water Resour 2019;126:116–28.
[52] Zhao J, Qin F, Derome D, Carmeliet J. Simulation of quasi-static drainage displacement in porous media on pore-scale: coupling lattice Boltzmann method and pore network model. J Hydrol 2020;588:125080.
[53] Zhao J, Qin F, Derome D, Kang Q, Carmeliet J. Improved pore network models to simulate single-phase flow in porous media by coupling with lattice Boltzmann method. Adv Water Resour 2020;145:103738.
[54] Aslannejad H, Samari-Kermani M, Nezami HM, Jafari S, Raoof A. Application of machine learning in colloids transport in porous media studies: lattice Boltzmann simulation results as training data. Chem Eng Sci 2022;253:117548.
[55] Rabbani A, Babaei M. Image-based modeling of carbon storage in fractured organic-rich shale with deep learning acceleration. Fuel 2021;299:120795.
[56] Rabbani A, Jamshidi S. Specific surface and porosity relationship for sandstones for prediction of permeability. Int J Rock Mech Min Sci 2014;71:25–32.
[57] Rabbani A, Jamshidi S, Salehi S. An automated simple algorithm for realistic pore network extraction from micro-tomography images. J Pet Sci Eng 2014;123:164–71.
[58] Benzi R, Biferale L, Sbragaglia M, Succi S, Toschi F. Mesoscopic modeling of a two-phase flow in the presence of boundaries: the contact angle. Phys Rev E 2006;74(2):021509.
[59] Zhang M, Liu Z, Pan B, Iglauer S, Jin Z. Molecular simulation on CO_2/H_2S co-adsorption in organic and inorganic shale nanopores. Appl Surf Sci 2023;624:157167.
[60] Dauber-Osguthorpe P, Roberts VA, Osguthorpe DJ, Wolff J, Genest M, Hagler AT. Structure and energetics of ligand binding to proteins: Escherichia coli dihydrofolate reductase-trimethoprim, a drug-receptor system. Proteins: Struct, Function, Bioinform 1988;4(1):31–47.
[61] Cygan RT, Liang J-J, Kalinichev AG. Molecular models of hydroxide, oxyhydroxide, and clay phases and the development of a general force field. J Phys Chem B 2004;108(4):1255–66.
[62] Martin MG, Siepmann JI. Transferable potentials for phase equilibria. 1. United-atom description of n-alkanes. J Phys Chem B 1998;102(14):2569–77.
[63] Potoff JJ, Siepmann JI. Vapor–liquid equilibria of mixtures containing alkanes, carbon dioxide, and nitrogen. AICHE J 2001;47(7):1676–82.
[64] Wang H, Huang J, Zhan S, Zhang M, Cai J. Study on CO_2 and CH_4 competitive adsorption in shale organic and clay porous media from molecular- to pore-scale simulation. SPE J 2024;SPE-219478-PA:1–13.
[65] Zhang M, Yang Y, Pan B, Liu Z, Jin Z, Iglauer S. Molecular simulation on H2 adsorption in nanopores and effects of cushion gas: implications for underground hydrogen storage in shale reservoirs. Fuel 2024;361:130621.
[66] Tian Z, Wei W, Zhou S, Wood DA, Cai J. Experimental and fractal characterization of the microstructure of shales from Sichuan Basin, China. Energy Fuel 2021;35(5):3899–914.
[67] Wang H, Wang W, Su Y, Jin Z. Lattice Boltzmann model for oil/water two-phase flow in Nanoporous media considering heterogeneous viscosity, liquid/solid, and liquid/liquid slip. SPE J 2022;27 (6):3508–24.